Title

Blood extracellular vesicles carrying synaptic function- and brain-related proteins as potential biomarkers for Alzheimers disease.

Journal

Alzheimers and Dementia, 19(3)

Authors

Tian, Chen

Stewart, Tessandra

Hong, Zhen

et al.

Publication Date

2023-03-01

DOI

10.1002/alz.12723

Peer reviewed

HHS Public Access

Author manuscript

Alzheimers Dement. Author manuscript; available in PMC 2024 January 02.

Blood Extracellular Vesicles Carrying Synaptic Function- and Brain-related Proteins as Potential Biomarkers for Alzheimer's Disease

Chen Tian, MD, PhD[1,2,*], **Tessandra Stewart, PhD**[2,*], **Zhen Hong, MD, PhD**[3,2], **Zhen Guo, MD**[1], **Patrick Aro, MS**[2], **David Soltys, BS**[2], **Catherine Pan, DDS**[1,2], **Elaine R Peskind, MD**[4,5], **Cyrus P. Zabetian, MD, MS**[6,7], **Leslie M. Shaw, PhD**[8,9], **Douglas Galasko, MD**[10], **Joseph F Quinn, MD**[11,12], **Min Shi, PhD**[2,†], **Jing Zhang, MD, PhD**[1,13,†] **Alzheimer's Disease Neuroimaging Initiative**

[1]Department of Pathology, First Affiliated Hospital, Zhejiang University School of Medicine, Zhejiang, Hangzhou, China

[2]Department of Laboratory Medicine and Pathology, University of Washington School of Medicine, Seattle, WA, USA

[3]Department of Neurology, West China Medical School, Sichuan University, Chengdu, Sichuan, China

[4]Department of Psychiatry and Behavioral Sciences, University of Washington School of Medicine, Seattle, WA, USA

[5]Northwest (VISN-20) Mental Illness, Research, Education, and Clinical Center, Veterans Affairs Puget Sound Health Care System, Seattle, WA, USA

[6]Veterans Affairs Puget Sound Health Care System, Seattle, WA, USA.

[7]Department of Neurology, University of Washington School of Medicine, Seattle, WA, USA.

[8]Center for Neurodegenerative Disease Research, Perelman School of Medicine at the University of Pennsylvania, Philadelphia, PA.

[9]Department of Pathology and Laboratory Medicine, Perelman School of Medicine at the University of Pennsylvania, Philadelphia, PA.

[10]Department of Neurology, University of California, San Diego, California, USA.

[11]Department of Neurology, Oregon Health & Science University, Portland, OR, USA

[12]Department of Neurology and Parkinson's Disease Research Education and Clinical Care Center (PADRECC), VA Portland Healthcare System, Portland, OR, USA.

[13]National Health and Disease Human Brain Tissue Resource Center, Zhejiang University, Zhejiang, Hangzhou, China

[†]Corresponding Author: Jing Zhang, MD, PhD, Department of Pathology, First Affiliated Hospital, Zhejiang University School of Medicine, Zhejiang, Hangzhou, China (jzhang1989@zju.edu.cn); or Min Shi, PhD, Department of Laboratory Medicine and Pathology, University of Washington School of Medicine, Seattle, WA, USA (mshi70@uw.edu).

[*]The authors contributed equally to this article.

Abstract

INTRODUCTION: Objective and accessible markers for Alzheimer disease (AD) and other dementias are critically needed.

METHODS: We identified NMDAR2A, a protein related to synaptic function, as a novel marker of CNS-derived plasma extracellular vesicles (EVs) and developed a flow cytometry-based technology for detecting such plasma EVs readily. The assay was initially tested in our local cross-sectional study to distinguish AD patients from healthy controls (HCs) or from Parkinson's disease (PD) patients, followed by a validation study using an independent cohort collected from multiple medical centers (the Alzheimer's Disease Neuroimaging Initiative or ADNI). CSF AD molecular signature was used to confirm diagnoses of all AD participants.

RESULTS: Likely CNS-derived EVs in plasma were significantly reduced in AD compared to HCs in both cohorts. Integrative models including CNS-derived EV markers and AD markers present on EVs reached Area Under Curve of 0.915 in discovery cohort and 0.810 in validation cohort.

DISCUSSION: This study demonstrated that robust and rapid analysis of individual neuron-derived synaptic function related EVs in peripheral blood may serve as a helpful marker of synaptic dysfunction in AD and dementia.

1. Narrative.

1.1 Contextual background

Alzheimer disease (AD) and related dementias are a major source of disability in the elderly, and the burden of these diseases on caregivers and the medical system is expected to increase as the population ages, especially in developed countries. For example, an estimated 6.2 million Americans age 65 and older are living with AD in 2021 in the United States (US), and the number is projected to reach 12.7 million by 2050. The estimated costs of AD in the US for health care, long-term care, and hospice are estimated at $355 billion in 2021 and is projected to be >$1.1 trillion in 2050 (in 2021 dollars) [1].

The molecular mechanisms underlying AD pathogenesis are incompletely defined, but amyloid beta (Aβ) peptides, derived from the amyloid precursor protein (APP), appear to be central to AD pathogenesis and are deposited in neuritic plaques found in the brains of AD patients. Tau protein is also crucially involved in AD pathogenesis; hyperphosphorylation, truncation, and oligomerization of tau are critical in the formation of neurofibrillary tangles, which constitute another pathological defining characteristic of AD. Together with the degeneration of neuronal cells, these pathological hallmarks have been conceptualized as a framework for identifying AD [2].

More recently, it has become clear that the fundamental pathological cause of the cognitive dysfunction associated with AD and other dementias appears to be the loss of neuronal synapses or of communication among the synapses, both of which occur at an early stage, in which neurons are injured, but not yet dead or dying. A range of synergistic mechanisms may contribute to such synaptic failure, possibly including alterations of normal APP regulation of presynaptic proteins, alterations in Ca^{2+} homeostasis, and altered function

and distribution of hyperphosphorylated tau[3, 4]. Other proposed mechanisms include genetic contributions, oxidative stress, and inflammation, among others [5–8]. Clearly defining molecular mechanisms of dementia is believed to be crucial in the development of therapies capable of preventing, slowing, or reversing the damage done to the brain during neurodegeneration.

Another major challenge in effective treatment of AD and related dementias is diagnosing them early and accurately, as the characteristic impairments in memory are often not identified in the clinic until after significant damage to the brain has already occurred. Further, it is very common for different types of dementia to appear clinically similar, especially at early stages, or for multiple types to occur simultaneously in the same patient. One approach to the diagnostic challenges is development of sensitive objective biomarkers. The best biomarker candidates to date rely on either relatively invasive methods (i.e., collection of cerebrospinal fluid or CSF obtained by lumbar puncture) or expensive tests (such as magnetic resonance imaging or positron emission tomography). These types of tests are often unacceptable, particularly during early stages when symptoms are not apparent, or inaccessible to patients. Thus, identification of non-invasive tests, such as reliable blood tests, are highly desired for those with mild symptoms or even those at asymptomatic, preclinical stages when neuroprotective therapies are likely to be most effective.

Additionally, many biomarker studies to date have focused on the two key proteins involved in the pathophysiology of AD: Aβ and tau. Tests measuring these proteins may reflect accumulation of pathological proteins (Aβ), neuronal death (tau, neurofilament), or changes in gross morphology associated with widespread damage (imaging), but modalities to reflect current or dynamic functional states are lacking. Thus, a marker capable of reporting the status of synaptic function might provide better information regarding not only the progression of the disease, but the engagement of putative medications with their targets, and the functional response of the targeted systems. Robust assays to measure these markers, preferably from a peripheral source such as blood, could be quite useful for both diagnostic and prognostic or monitoring purposes.

Unfortunately, because the brain is protected by a system of cellular interactions termed the blood-brain barrier (BBB), which prohibits the diffusion of macromolecules to blood, it is difficult to monitor the brain via peripheral fluids. Enormous efforts have been diverted to identify blood-based biomarkers for AD and related disorders; however, only limited success has been achieved. While some molecules, including Aβ and tau, are shuttled across the BBB and into the periphery via transport mechanisms that are not yet well-characterized, these brain-derived molecules are often either indistinguishable from those generated by peripheral systems, or are present in such low abundance that they cannot be identified within the extremely complex molecular milieu of the blood. In the last year or so, several blood-based assays have been introduced, demonstrating promising results in differentiating AD from controls, although validation by additional independent groups is still critically needed [9, 10].

Increasing evidence has suggested that some of the molecules exported from the brain are carried within extracellular vesicles (EVs), including exosomes [11–13]. EVs are

membrane-bound, circulating compartments secreted by most cell types, and carry cargo generated by the parent cells. They play important roles in communication between cells, and can alter the behavior of downstream target cells. Because they also carry protein markers that identify the type of cell from which they were secreted, and can cross from the brain into the circulation, they provide a subpopulation of brain-derived molecules that can be enriched from the peripheral circulation (i.e., blood), isolated, and measured, with reasonable confidence in their origin.

Recently, we and others have developed new strategies for measuring biomarkers for AD and other neurodegenerative disorders by targeting EVs carrying proteins that mark them as derived from the brain or nervous system [11, 14–17]. These EVs can be purified or identified by targeting the cell type marker protein, and mechanistically interesting cargo can be measured, allowing the quantification of brain target biomarkers, without requiring invasive or expensive tests. Promising results demonstrating differences in EV-associated markers for AD were reported in multiple independent studies[15, 16, 18–22]; however, many of these studies were conducted in small cohorts and the procedures were relatively labor-intensive and could be difficult to follow, and thus further confirmation and validation are still needed.

1.2 Study design and main results

In this study, we mainly focused on *N*-methyl-*D*-aspartate (NMDA) receptor 2A (NMDAR2A, or GRIN2A), a protein closely relating to neuronal synaptic function and a current therapeutic target of Memantine, and L1CAM, a neuronal marker identified by us previously[11], to measure the number and cargo content of potential brain-derived EVs in the plasma of AD patients, as well as patients with Parkinson's disease (PD) and age-matched neurologically healthy controls (HCs). We used a highly sensitive microscopy technique to show that both of these markers are present on EVs. For a more practical use of markers, we then optimized a sensitive and rapid flow cytometry-based technology (Apogee) we recently developed for measurements of CSF EVs[23] to analyze individual EVs in blood for improved biomarker accuracy and utility. In the Apogee system, target protein (EV surface marker) is labeled with fluorescent antibodies, and the number of EVs carrying the target is quantified.

The EV markers were measured first in a discovery cohort, consisting of patients with AD, PD, and neurologically healthy age- and sex-matched control subjects. The encouraging results obtained in this local cohort were then largely confirmed in a second, validation cohort, consisting of AD patients and HC subjects from the Alzheimer's Disease Neuroimaging Initiative (ADNI) study, with the contribution of the samples from many different hospitals throughout the US. CSF data collected in previous studies was used to ensure that subjects included in the current work had CSF Aβ and tau profiles that matched their reported diagnoses.

We found that there were significantly fewer EVs carrying either of the potential brain markers, NMDAR2A and L1CAM, in plasma from AD subjects compared to controls or PD patients. When we used either the NMDAR2A+ or L1CAM+EVs alone, or a combination of the number of brain-derived EVs and EVs carrying AD-related proteins, we were able

to distinguish AD patients from controls, with the combined markers performing best in separating the groups. This model worked in the discovery cohort with relatively high sensitivity and specificity, but less well in the ADNI cohort. Of note, while not reaching the ideal degree of separation in the validation cohort, the EV markers performed better than most previously examined peripheral markers.

1.3 Study conclusions, potential clinical applications, and other implications

We identified a novel marker of brain-derived EVs, NMDAR2A, which likely reflects the state of synaptic function in the brain, using plasma samples and a robust flow cytometry-based assay. Although these results are preliminary, this assay has the potential to become a useful tool in clinical settings. Because it may reflect the process of neuronal synaptic loss more directly than current assays, it could prove a sensitive and rapid diagnostic test, capable of predicting cognitive impairment in AD or other dementias or even detecting these disorders at a stage where neurons are damaged and functioning poorly, but not yet dying. An additional benefit could be utility in selecting subjects for future clinical trials, ensuring that novel therapeutics are tested in suitable candidates, rather than in highly heterogeneous populations seen at most clinics.

Among all markers tested, NMDAR2A was most capable of distinguishing AD from the other diagnostic groups (PD or healthy controls). This finding is of particular interest, because of the role of NMDAR2A in the brain. This protein is a receptor for the neurotransmitter glutamate, and it has key roles in such processes as long-term potentiation, a strengthening of synaptic interactions important in learning and memory[24–27]. Changes in NMDA receptors occur early in the processes underlying AD, and reducing NMDA activity is one of the current strategies to treat AD[27–29]; thus, the new assay described here may serve as a non-invasive proxy for a brain mechanism closely related to dementia/cognitive impairment.

Another important result was L1CAM behaved similarly to NMDAR2A in AD compared to control patients. Some controversy exists regarding the use of L1CAM as a neuronal marker, as it is known to be expressed in some specialized and cancer cell types. Our experiments using a robust microscopy technology clearly demonstrated that both neuronal markers can be observed on the surface of EVs, alongside general EV identity markers, and their similar performance suggests that both markers represent a population enriched for CNS- or neuron-derived EVs.

The flow cytometry-based assay used here (and in our recent CSF study[23]) also addressed an additional challenge of early L1CAM studies: the complicated procedures required to isolate the EVs. These sensitive and rapid assays directly quantify intact, individual EVs, without extensive purification before quantifying AD markers. This approach bypasses some issues of EV isolation, potentially reducing inter-lab variability and increasing the clinical utility of EV-based biomarkers.

1.4. Limitations, unanswered questions, and future directions

One major question that remains is whether these specific biomarkers could be used for diagnosis in a clinical setting, and replication in larger cohorts is necessary to determine

this. Our cohorts had the advantage of available CSF measurements, allowing us to identify the most likely true AD cases, vs those with clinically similar dementias. While this is a strength of the study, allowing for the assessment of the assay in the population of interest (AD), the assay performance in a mixed population, more similar to the population seen in clinics, remains to be determined. Ideally, this should be carried out via large, multi-site studies in well-characterized subjects, with the samples collected using a robust protocol. In this study, samples were collected in the two cohorts following slightly different protocols, which might account for some of the differences observed within the same diagnostic groups across the cohorts.

An equally important question is whether these EV markers could serve as an index to predict clinically meaningful characteristics of AD and other dementias, such as problems with memory or function, which is believed to be more important than just detection of the disease[30]. Identification of surrogate markers for synaptic dysfunction/degeneration is of fundamental importance, particularly in the development of novel therapeutics, for which suitable surrogate markers that can report pathologically meaningful changes in the brain, as well as predict clinically meaningful changes in cognition, is necessary to improve the testing and approval of novel treatments. Further, the available cognition measures tend to report relatively more severe impairment, and are not sensitive enough to detect the earliest stages of decline, where a marker of synaptic failure would be of the greatest utility. The findings of NMDAR2A-carrying EVs in the present study are thus of particular interest, due to the potential association of these EVs with the state of synaptic function in the brain. In future studies, whether NMDAR2A-positive EVs in plasma may serve as such a marker to predict cognitive impairment or memory loss should be determined. Such studies would ideally follow subjects longitudinally, to determine whether these markers predict/trace progressive impairment, and whether the association persists beyond the stage of synaptic dysfunction, or reaches a plateau as neurons are lost. Moreover, whether these markers could be used for early detection of cognitive impairment in AD and related dementias should be studied by measuring their levels in very early disease and even patients at risk of developing disease, to determine whether they have prognostic value, because synaptic loss is believed to start in early stages of AD, like those with mild cognitive impairment (MCI).

Another important unanswered question is whether the identified EV markers are specific to AD, or appear in other neurological conditions, with or without dementia. In this study we observed differences in the number of brain-derived plasma EVs when comparing AD and PD, but these markers, particularly NMDAR2A-carrying EVs, might serve as a more general marker of synaptic failure in different types of cognitive impairment/dementia. Future studies should not only replicate the AD vs PD finding, but also include subjects with other types of dementia and neurological conditions (e.g., patients with frontotemporal dementia, PD dementia, or dementia with Lewy bodies), to determine how specific the effect is to AD and/or dementia. Ideally, a peripheral biomarker such as those we are proposing here would also be useful in tracking progression, or even recovered/preserved function with implementation of novel therapies. These uses are not addressed in the present study, and must be examined by repeated measurement in longitudinal studies.

Relatedly, the present study demonstrated that the number of probable neuronal EVs carrying several markers were all lower in AD compared to the other groups. Several potential explanations might be consistent with this observation. For example, it may be a result of the loss of neurons to produce them. Conversely, it is possible that AD affects the EV-producing or exporting cellular machinery (for shunting pathological proteins out of neurons and into the peripheral circulation) more broadly. To test these hypotheses, further examination of EV-related processes throughout the course of AD will be required to fully elucidate the cause of the changes in the EV population observed here. Future studies should also compare the number of EVs from other cellular sources and bodily systems, to see if they are also altered in AD patients. Notably, no such decrease was observed in PD subjects, despite that PD also features the death of neurons, and the reasons for this should also be identified. Some possibilities might be the difference in the cell type, affected brain regions, or distribution of affected cells, or that the diseases differentially affect the mechanisms by which the particles of interest exit the brain.

Another set of questions that must be answered relates to the preliminary status of NMDAR2A as a novel marker of synaptic function and brain/neuron-derived EVs. The correlation of the number of NMDAR2A+ EVs with cognitive function in patients and with synaptic degradation based on pathological analysis of tissue should be measured, and the observed changes of these EVs in AD need to be confirmed in animal models. Moreover, the transportation of NMDAR2A+ EVs from the brain into peripheral blood also needs to be confirmed in animal studies. The specificity of these EVs for the brain should be further confirmed, probably by examining the presence of NMDAR2A in conjunction with proteins that are present on EVs (e.g., tetraspanins), and lack of expression on other EV types. However, communication among different CNS cells via EVs, a phenomenon increasingly recognized recently[31–35], might make this approach more complicated. It is notable that this preliminary study has shown a similar performance to some of the best plasma assays to-date, including those using extremely sensitive assays of tau proteins[36]. Importantly, the assay is capable of identifying multiple markers simultaneously, and whether other combinations of markers related to different processes might further improve the performance will be an important addition to future studies.

Additional technical limitations and caveats related to the methods used in this study are discussed in the Detailed Results below (section 3.2).

2. Consolidated Results and Study Design

This is a multi-center study including a discovery cohort and a validation cohort. The discovery cohort included 88 patients with AD, 84 patients with PD, and 99 age- and sex-matched (frequency matching) HCs, enrolled in the University of Washington Alzheimer's Disease Research Center (UW ADRC) or the Pacific Northwest Udall Center of Excellence in PD Research (PANUC). The validation cohort included 100 patients with AD and 100 HCs with a similar distribution of age and sex, and was obtained from the ADNI. In some analyses, previously obtained values for CSF Aβ and tau were used to further select a subset of the subjects such that only those patients with a clinical diagnosis of AD and a CSF

signature consistent with AD were included in the “AD” group, and only subjects with no clinical diagnosis and no CSF signature typical to AD were considered “control”.

First, we identified NMDAR2A as another, possibly more CNS-specific (proteinatlas.org) EV marker compared to previously identified L1CAM. These neuronal markers were confirmed to be present on the surface of EVs using stochastic optical reconstruction microscopy (STORM), a microscopy technique capable of imaging individual EVs. Ultracentrifuged plasma EVs were analyzed by imaging the co-localization of either NMDAR2A or L1CAM with a general marker of EVs, or with AD-related markers ($A\beta_{42}$, $A\beta_{40}$, pTau231, or pTau396). Each of these markers were identified in close proximity to the marker of putative neuronal EVs, indicating that the neuronal EV markers are indeed present on EVs, and the AD-related markers are present on these likely neuronal EVs.

Next, nanoscale flow cytometry (Apogee) assays that we previously developed in CSF[23] were optimized to measure NMDAR2A+, L1CAM+ and AD marker+ EVs in blood plasma. We then used the optimized assay to examine individual samples for discovery cohort subjects meeting the CSF t-tau/$A\beta_{42}$ cutoff identified previously[37, 38] to select “true” AD and HCs. EVs carrying each marker were quantified as a ratio of all EVs, and the levels compared between groups. The ability of these values to distinguish between groups was assessed by generating receiver operating characteristic (ROC) curves.

There were no differences in the total number of EVs detected in plasma between AD and control subjects. The number of EVs carrying NMDAR2A+ and L1CAM+ EVs were lower in AD vs HCs. Levels of $A\beta_{40}$+, $A\beta_{42}$+, p-Tau231+ and p-Tau396+ EVs were also lower in AD than HCs. To help distinguish AD-specific effects from general effects of neurodegenerative disease, PD patient plasma samples were also examined as a neurodegeneration control. AD levels of L1CAM+, $A\beta_{40}$+, $A\beta_{42}$+, pTau231+, and pTau396+ EVs were lower than in PD.

ROC analysis was then performed to evaluate the ability of the selected markers to distinguish between groups. In comparing AD and HC, the sensitivity and specificity for NMDAR2A+ EVs were 82% and 81% [AUC=0.89, 95% confidence interval (CI) 0.82–0.96] and 51% and 91% (AUC=0.779, 95% CI=0.68–0.88] for L1CAM+ EVs. The markers only had moderate ability to distinguish between AD and PD. An integrative model combining all EV markers discriminated AD from HCs with an AUC of 0.915 (95% CI=0.86–0.97; sensitivity=85%, specificity=84%).

To validate these results, ADNI baseline samples from CSF t-tau/Aβ42 confirmed cases were also assessed. Group differences between AD and HCs were confirmed for total particles and all markers. Similar group differences between AD and HCs observed in the discovery cohort were confirmed for all markers. In the validation cohort, the ability of NMDAR2A- and L1CAM-positive EVs to distinguish AD patients from healthy controls was also assessed; the sensitivity and specificity were 74% and 67% (AUC=0.809, 95% CI=0.74–0.88) for NMDAR2A+ EVs, 72% and 70% (AUC=0.762, 95% CI=0.69–0.84) for L1CAM+ EVs. Intriguingly, the integrative model performed well in the validation cohort,

distinguishing AD from HC with a sensitivity and specificity of 81% and 63% (AUC=0.810, 95% CI=0.74–0.88).

3. Detailed Methods and Results

3.1 Methods

3.1.1 Participants and sample collection—All procedures were approved by the respective Institutional Review Boards, and each subject provided informed consent. The discovery cohort included 88 patients with AD, 84 patients with PD, and 99 age- and sex-matched (frequency matching) HCs, enrolled in the UW ADRC or PANUC. When CSF AD molecular signature was used to select "true" AD and HCs, 45 AD and 32 HCs met the CSF t-tau/$A\beta_{42}$ cutoff identified previously[37, 38](Table 1). All participants underwent extensive clinical evaluation, and the inclusion and exclusion criteria as well as sample collection procedures have been previously described[11, 14, 23, 38, 39].

The validation cohort included 100 patients with AD and 100 HCs with a similar distribution of age and sex, and was obtained from ADNI[40]. The inclusion and exclusion criteria have been described previously and can be found on the ADNI website (adni.loni.usc.edu). The diagnoses of 66 AD and 82 HC participants were confirmed using previously published cutoffs for ratios of CSF t-tau/Aβ42 [41] (Table 1); AD subjects were included for the analyses if their ratios met the cutoff of AD diagnosis, and control subjects were included if their ratios did not.

Reference plasma samples (each pooled from 10–30 healthy controls) were obtained at the University of Washington as described previously[11, 14, 42].

3.1.2 Plasma sample processing—Plasma samples were thawed rapidly at 37°C and centrifuged at 3000 × *g* for 30 min (4°C), followed by 10,000 × *g* for 30 min (4°C). 100 μL of cleared plasma was diluted with 1,000 μL of phosphate-buffered saline (PBS; 0.22 μm-filtered) and then centrifuged at 100,000 × *g* for 1h at 4°C. Pellets were resuspended in ~1 mL of filtered PBS and centrifuged again at 100,000 × *g* for 1h at 4°C. The pelleted EVs were then resuspended in ~200 μL of filtered PBS and stored at −80°C before use.

3.1.3 Stochastic optical reconstruction microscopy (STORM)—All images were acquired on a Nikon N-STORM super-resolution system (Nikon Instruments Inc.) with a Nikon Eclipse Ti inverted microscope and a 100×TIRF lens (numerical aperture 1.49). The 561 nm semiconductor laser was used to excite fluorophores of Alexa 561, The 488 nm semiconductor laser was used to excite fluorophores of Alexa 488, The 647 nm semiconductor laser was used to excite fluorophores of Alexa 647, and the lower 405 nm laser was used to increase the number of on-state fluorophores according to general recommendation. 2,000 frames with a 60 ms exposure time were recorded to image one cell by an electron multiplying CCD camera (Andor ixon DU-897). The capture time of one cell was usually about 20 min. During the fluorescence acquisition, Nikon microscopic imaging device provided a Perfect Focus System (PFS) to achieve real-time correction of focus drift in Z axis direction.

Ultracentrifuged plasma EVs were washed three times with PBS and then immersed in 200 μl of a buffer specialized for STORM imaging [7 μL of oxygen-scavenging GLOX buffer (14 mg of glucose oxidase, 50 μL of 17 mg/mL catalase in 200 μL of 10 mM Tris, 50 mM NaCl, pH 8.0), 70 μL of MEA buffer (1M), plus 620 μL of Buffer B (50 mM Tris-HCl (pH8.0), 10 mM NaCl, 10% Glucose)] before data acquisition.

3.1.4 Electron Microscopy (EM)—Five μL ultracentrifuged reference plasma, prepared identically to the cohort samples, were deposited on an EM grid coated with a perforated carbon film and incubated for 30 minutes; the liquid was blotted from the back side of the grid and the grid was quickly plunged into liquid ethane using a Leica EMCPC cryo-chamber. EM grids were stored under liquid nitrogen prior to EM observation. Cryogenic EM (Cryo-EM) was performed with a Titan Krios electron microscope (ThermoFisher, USA).

3.1.5 Nanoparticle Tracking Analysis (NTA)—NTA was performed using a NanoSight NS300 instrument with a 405 nm violet laser (Malvern, UK) according to the manufacturer's instructions. Briefly, 10 μL ultracentrifuged reference plasma were diluted 1:100 with 0.22 μm-filtered PBS (pH 7.4) to a final volume of 1 mL for direct scatter measurement. Ideal measurement concentrations were identified by pre-testing the ideal particle per frame value (20–100 particles/frame). The ideal detection threshold was determined to include as many particles as possible with the restrictions that 10–100 red crosses were counted while only <10% were not associated with distinct particles. For each measurement, five 1-min videos were captured under the following conditions: cell temperature: 25°C; Syringe speed: 40 μL/s. The videos were analyzed using NanoSight Software NTA 3.1 Build 3.1.46 with a detection threshold of 5.

3.1.6. EV analysis with Apogee nanoscale flow cytometry—Fluorophore-conjugated antibodies were generated by using Zenon IgG labeling kits (Invitrogen/Life Technologies, Carlsbad, CA, USA) according to the manufacturer's protocol. Specifically, mouse anti-L1 cell adhesion molecule (L1CAM) monoclonal antibody (80832, Abcam) was labeled with the Zenon Alexa Fluor 405 mouse IgG_1 labeling kit; and mouse anti-N-methyl-D-aspartate (NMDA) receptor subunit 2A (NMDAR2A) monoclonal antibody (MA5-27693, Thermo Fisher Scientific) was labeled with Zenon Alexa Fluor 405 mouse IgG_{2b} labeling kit. Mouse anti-$A\beta_{40}$ monoclonal antibody (805401, BioLegend) was labeled with the Zenon Alexa Fluor 647 mouse IgG_1 labeling kit; and rabbit anti-$A\beta_{42}$ monoclonal antibody (700254, Thermo Fisher Scientific) was labeled with the Zenon Alexa Fluor 647 Rabbit IgG labeling kit. Mouse anti-p-Tau231 monoclonal antibody (MN1040, Thermo Fisher Scientific) was labeled with the Zenon Alexa Fluor 647 mouse IgG_1 labeling kit; and mouse anti-p-Tau396 monoclonal antibody (35–5300, Thermo Fisher Scientific) was labeled with the Zenon Alexa Fluor 647 mouse IgG_{2b} labeling kit.

Immunoglobulin isotype controls of corresponding species were also labeled at the same final concentrations as all the antibodies. Another negative control (no antibody "Blank", i.e., dye only) was the use of the same volume of PBS instead of specific antibodies during the labeling reaction.

Labeled anti-L1CAM or anti-NMDAR2A (Alexa Fluor 405 labeled), together with another Alexa Fluor 647 labeled antibody ($A\beta_{40}$, $A\beta_{42}$, p-Tau231, or p-Tau396), were added to 10 μL of ultracentrifuged plasma sample (equivalent antibody amount per sample: 0.1 μg) and incubated overnight at 4°C. Labeled sample was then fixed with 20 μL of 0.22μm-filtered 4% PFA for 20 min at room temperature.

Samples were analyzed using an Apogee Micro-PLUS flow cytometer (Apogee Flow Systems, Hemel Hempstead, UK) with a 70 mW 405 nm laser for light scattering in forward and side directions and blue fluorescence and a 200 mW 488 nm laser for green fluorescence as previously described[23]. Under the optimized micro-flow cytometry settings, the sample maintains a stable particle number count and no aggregation. Apparent sample concentrations showed dilution linearity following dilution of the sample. The reference beads and EV samples were run at the following high-threshold settings (minimizing background noise): the threshold numerical values for lasers 405-LALS and 405-Blue were set at 17 and 25, respectively; the numerical value and voltage for laser 405-Blue were set at 1 and 450 V, respectively. The sheath fluid pressure was set at 150 mbar and samples were introduced at a flow rate of 1.5 μL/min.

All samples were kept at 4°C and tested within 8 hours after labeling, and labeling was stable under these conditions. For each cohort, clinical samples were analyzed in a single batch in two days, and samples from different diagnostic groups were distributed across each day. Two reference plasma samples, pooled from ~30 HCs, were added into each day's measurements to help to assess day-to-day variations (<5%).

3.1.7 CSF protein measurements—CSF $A\beta_{42}$, total tau (t-tau), and phosphorylated tau (p-tau181) in the discovery cohort were measured by using the INNO-BIA AlzBio3 Luminex assay (Innogenetics, Ghent, Belgium) and were published previously[37, 38]. Values for these CSF proteins in the ADNI cohorts measured with Roche Elecsys assays were obtained from the ADNI database (adni.loni.usc.edu).

3.1.8. High-density lipoprotein (HDL) and low-density lipoprotein (LDL) measurements—LDL and HDL levels in plasma samples, including whole plasma, ultracentrifugation-enriched plasma EVs, and EV-poor plasma (supernatant after ultracentrifugation), were measured with a Roche Cobas c701 automatic analyzer (Roche Diagnostics, Mannheim, Germany). All testing reagents, including calibrators and controls, were supplied by Roche Diagnostics. 200 μL of each sample were used for LDL and HDL measurements.

3.1.9 Statistical analysis—All analyses were performed in SPSS 25.0 (IBM, Chicago, IL, USA) or Prism 8.0 (GraphPad Software, La Jolla, CA, USA). The normality of distribution of dataset was analyzed (Shapiro-Wilk test). Mann–Whitney U test (for two groups) or one-way non-parametric ANOVA, Kruskal-Wallis test (for three groups) were used to compare group mean total particle number detected by scatter (independent of any fluorescent cell type label), or ratio of a given positive marker to total events. ROC curves for analytes were generated to evaluate their sensitivities and specificities in distinguishing

AD from HCs or PD. Logistic regression was used to generate an integrative model that included multiple plasma biomarkers. $P<0.05$ was regarded as significant.

3.2 Results

EVs to be examined in this work were characterized following their enrichment from plasma via ultracentrifugation according to MISEV2018 recommendations [43]. To analyze their morphology and size, we performed cryo-EM analysis of the EVs after ultracentrifugation. We were able to detect double membrane structured EVs with a diameter of around 150 nm (Fig. 1). NTA was further used to determine the sizes and distribution of EVs, showing a broad peak with a maximum around 70 nm. We also analyzed EV-specific markers by western blot. As expected, western blot analyses demonstrated that EV samples from ultracentrifugation were enriched for NMDAR2A as well as general EV markers Alix and CD9 proteins. To determine whether this process enriched other lipid-containing particles, we also used immunoassays to analyze the content of raw plasma, ultracentrifugation-enriched EVs, and EV-poor plasma (supernatant after ultracentrifugation) for lipoproteins, and found that the majority of HDL and LDL remained in the supernatant after centrifugation (Fig. 1).

Previous studies by us and others used L1CAM as a marker for CNS/neuron-derived EVs[11, 14, 19]. In this study, we further identified NMDAR2A as another, possibly more CNS-specific (proteinatlas.org) EV marker. STORM, a super-resolution microscopy technique for single-molecule imaging, was performed to confirm L1CAM or NMDAR2A and EV general marker CD9 presence together on EV membranes. Nanoscale sized fluorescent beads with a diameter of 100 nm were included as a scale standard. To confirm the EV identity of the detected signal in ultracentrifuged plasma samples, L1CAM or NMDAR2A was compared with the EV marker CD9 on the EV membranes together (Fig. 2A). Colocalization of NMDAR2A or L1CAM together with general EV marker (CD9), on the same plasma EVs surface was observed. Colocalization of NMDAR2A or L1CAM together with pTau231 or pTau396, along with a general EV marker (CD9), on the same plasma EVs surface was also confirmed using STORM technology (Fig. 2B). Additionally, we found that NMDAR2A or L1CAM together with $A\beta_{40}$ or $A\beta_{42,}$ and CD9 were on the same plasma EVs surface by STORM technology (Fig. 2C).

Nanoscale flow cytometry (Apogee) assays that we previously developed in CSF[23] were optimized to measure NMDAR2A+, L1CAM+ and AD marker+ EVs in plasma. Assay specificities and dilution linearity were confirmed (Fig. 3). A single reference plasma sample was run in duplicate, repeated over five days, to demonstrate the day-to-day stability. Coefficients of variation for intra- and inter-day assay comparisons were ≤ 10% for all markers. Reference standards (fluorescent beads of known size) were run regularly to calibrate Apogee performance (Fig. 4A). The relationship between total gated positive events and sample dilution is presented in Fig. 4B, to address the coincidence of events by swarming.

Next, we examined individual samples for discovery cohort subjects meeting the CSF t-tau/$A\beta_{42}$ cutoff identified previously [37, 38] to select “true” AD and HCs. There were no differences in the total number of EVs detected in plasma between AD and control subjects

(mean number of total particles detected by scatter, regardless of fluorescence; p=0.21, Kruskal-Wallis, Supplemental Fig. 1). Moreover, no differences were observed in either large or small particles when particles above vs below 150 nm were analyzed separately (Supplemental Fig. 1). Further, because Apogee technology cannot detect the particles smaller than 80 nm readily, an NTA analysis was performed in a small cohort of 30 AD and 30 controls, showing no significant difference in total particle number or number of exosome-size (40–150 nm) particles vs larger (>150 nm) particles (Supplemental Table 1).

More interestingly, levels of NMDAR2A+ and L1CAM+ EVs were lower in AD vs HCs in the discovery cohort (Table 1; Fig. 5 A–B) and this trend was the same in small (≤150 nm) and larger (>150 nm) EVs (Supplemental Fig. 2). Levels of $A\beta_{40}$+, $A\beta_{42}$+, p-Tau231+ and p-Tau396+ EVs were also lower in AD than HCs (Table 1; Fig. 5C–F). As neurodegenerative disease controls, PD patient plasma samples were also examined; AD levels of L1CAM+, $A\beta_{40}$+, $A\beta_{42}$+, pTau231+, and pTau396+ EVs were lower than in PD (Fig 5A–F). Marker levels did not correlate with age; however, correlations were observed between markers (Table 2).

ROC analysis was then performed to evaluate diagnostic performance. In comparing AD and HC, the sensitivity and specificity for NMDAR2A+ EVs were 82% and 81% [AUC=0.89, 95% confidence interval (CI) 0.82–0.96] and 51% and 91% (AUC=0.779, 95% CI=0.68–0.88] for L1CAM+ EVs (Fig. 5G). For other EV markers, and PD vs AD, the performance was moderate (Table 3). However, an integrative model combining all EV markers (Fig. 5H) discriminated AD from HCs with an AUC of 0.915 (95% CI=0.86–0.97; sensitivity=85%, specificity=84%). EVs carrying Aβ and or Tau species, alone or in combination with NMDAR2A or L1CAM, did not further increase the diagnostic power over NMDAR2A or L1CAM.

To validate these results, ADNI baseline samples from CSF t-tau/$A\beta_{42}$ confirmed cases were also assessed. Group differences between AD and HCs were confirmed for total particles (p=0.58, Mann–Whitney) and all markers (Table 1; Fig. 6A–F). The sensitivity and specificity were 74% and 67% (AUC=0.809, 95% CI=0.74–0.88) for NMDAR2A+ EVs, 72% and 70% (AUC=0.762, 95% CI=0.69–0.84) for L1CAM+ EVs (Fig. 6G). Intriguingly, the integrative model (Fig. 6H) distinguished AD from HC with a sensitivity and specificity of 81% and 63% (AUC=0.810, 95% CI=0.74–0.88).

It should be noted that, in addition to NMDAR2A- and L1CAM-carrying EVs, in this study we also investigated EVs carrying traditional AD biomarkers (Aβ and tau). For Aβ, it has been reported that some cleavage of amyloid precursor protein to Aβ peptides have been found to occur in the endosome, and some Aβ peptides are released from cells in association with exosomal membranes[44]. Aβ peptides are thus commonly detected in EVs, particularly on the surface of EVs[45], from the CSF and blood of AD patients [46]. In contrast, although tau has been reported to be secreted into EVs and its disease-associated phosphoforms are enriched in EVs from AD CSF [44], the presence of p-tau species on the surface of EVs appears to be counterintuitive because they are typically considered intracellularly distributed. Though more details remain to be investigated, one possibility is that intracellular proteins are flipped along with the membrane when EVs are formed. Yet,

the “flipping” hypothesis is not applicable to all proteins because monomeric or oligomeric α-synuclein, proteins investigated in our recent manuscript, cannot be detected until the EVs are permeated [23]. Clearly, more studies are needed to characterize EVs, especially those related to neurodegenerative disorders.

Our study adds to a growing literature of biomarkers for AD carried on or within EVs. Several previous studies have reported levels of classical AD-related proteins, including Aβ species as well as total and phosphorylated tau species, indicating increased levels of these markers in brain-derived plasma EVs[15, 21, 47, 48], but the results on total tau levels in such EVs have been inconsistent[14, 15, 21, 22, 49]. Notably, each of these studies quantified the concentration of target proteins in a sample of lysed EVs isolated from the plasma via immunocapture. In contrast, the fluorescent label and flow cytometry method used here quantifies the number of intact EVs carrying the marker of interest; thus, although we observed a decrease in EVs carrying these markers, the results do not necessarily conflict with previous works. Notably, similar studies focusing not on classical AD markers, but on synaptic proteins, have frequently observed decreased levels, possibly reflecting the loss of synapses characteristic of neurodegeneration[47, 50–52]. Further studies are needed to confirm whether potentially brain-derived EV levels, specific marker levels contained in each EV, or both, are changed in AD.

Additionally, several technical caveats must be considered regarding these detailed results. The current Apogee system may not detect EVs <100 nm accurately, and complementary technologies are required in future studies to examine smaller EVs precisely. Additionally, because the isolation technique used to enrich the EVs from plasma, ultracentrifugation, in this study is known to sometimes cause particles to aggregate, it is possible that the imaging data showing that these neuronal markers co-localized with general EV markers may have actually represented two separate EVs, each with one of the markers, closely associated with each other. These possibilities can be distinguished in future experiments using a label to mark the interior of the EVs, as a contrast to the membrane labels used in the present study. Finally, the variability between subjects in total EVs, as well as the difficulty in ensuring specificity for EVs in measures of plasma particles, make normalization of the marker-positive EVs both necessary and challenging. Here, we have addressed the issue by normalizing positive EVs to all detected particles, accounting for variation by reporting the positive ratio. A more rigorous control would be to normalize to a fluorescent marker that labels all EVs (and only EVs); however, such specific markers are lacking. Tetraspanins, e.g. CD9 used in our STORM study, the most widely used EV markers, label only a subset of probable EV particles[53, 54], making them unsuitable as a total marker. Thus, identification of such universal EV markers in the future will improve further studies of EVs.

Supplementary Material

Refer to Web version on PubMed Central for supplementary material.

Funding/Support

This study was supported by National Institutes of Health (R01 AG056711, U01 NS091272, R21 AG060142, and R21 NS104511 to J.Z. and M.S., R21/R33 MH118160 to J.Z. and T.S., R01 AG061383 and RF1 AG068406 to

M.S., P50 NS062684 to C.P.Z., and P50 AG05136 to E.R.R). This study was also supported by National Key Technology Research and Development Program of China (No. 2016YFC1306500), Natural Science Foundation of China (International (Regional) Cooperation and Exchange Project, 82020108012), Innovation translational research fund of Zhejiang University for Year 2020, and National Health and Disease Human Brain Tissue Resource Center Construction National Ministry of Science and Technology Project for the STORM study and part of C.T. and Z.G.'s efforts. C.T. was also supported by China Postdoctoral Science Foundation (2021M702829) and Fundamental Research Funds for the Central Universities (2021FZZX005-27). It is also the result of work supported with resources and the use of facilities at the Veterans Affairs Puget Sound and Veterans Affairs Portland Health Care Systems. The content is solely the responsibility of the authors and does not necessarily represent the official views of the sponsors. The authors thank Dr. Wei Yin and the core facility platform at Zhejiang University School of Medicine for STORM technical support and analysis. The authors also deeply appreciate the participants who donated their blood for this study.

Role of the Funder/Sponsor:

The funding sources had no role in the design and conduct of the study; collection, management, analysis, and interpretation of the data; preparation, review, or approval of the manuscript; and decision to submit the manuscript for publication.

References

1. Association A.s., 2021 Alzheimer's Disease Facts and Figures. Alzheimers Dement, 2021. 17(3): p. 79.
2. Jack CR Jr., et al. , NIA-AA Research Framework: Toward a biological definition of Alzheimer's disease. Alzheimers Dement, 2018. 14(4): p. 535–562. [PubMed: 29653606]
3. Barthet G and Mulle C, Presynaptic failure in Alzheimer's disease. Prog Neurobiol, 2020. 194: p. 101801. [PubMed: 32428558]
4. Jordà-Siquier T, et al. , APP accumulates with presynaptic proteins around amyloid plaques: A role for presynaptic mechanisms in Alzheimer's disease? Alzheimers Dement, 2022.
5. Vaillant-Beuchot L, et al. , Accumulation of amyloid precursor protein C-terminal fragments triggers mitochondrial structure, function, and mitophagy defects in Alzheimer's disease models and human brains. Acta Neuropathol, 2021. 141(1): p. 39–65. [PubMed: 33079262]
6. Kowalska M, et al. , Genetic Variants and Oxidative Stress in Alzheimer's Disease. Curr Alzheimer Res, 2020. 17(3): p. 208–223. [PubMed: 32091332]
7. Zhou J, et al. , Imbalance of Microglial TLR4/TREM2 in LPS-Treated APP/PS1 Transgenic Mice: A Potential Link Between Alzheimer's Disease and Systemic Inflammation. Neurochem Res, 2019. 44(5): p. 1138–1151. [PubMed: 30756214]
8. Li Z, et al. , Astrocytes deliver CK1 to neurons via extracellular vesicles in response to inflammation promoting the translation and amyloidogenic processing of APP. J Extracell Vesicles, 2020. 10(2): p. e12035. [PubMed: 33408815]
9. Karikari TK, et al. , Blood phosphorylated tau 181 as a biomarker for Alzheimer's disease: a diagnostic performance and prediction modelling study using data from four prospective cohorts. Lancet Neurol, 2020. 19(5): p. 422–433. [PubMed: 32333900]
10. Tijms BM and Teunissen CE, Concatenating plasma p-tau to Alzheimer's disease. Brain, 2021. 144(1): p. 14–17. [PubMed: 33578422]
11. Shi M, et al. , Plasma exosomal alpha-synuclein is likely CNS-derived and increased in Parkinson's disease. Acta Neuropathol, 2014. 128(5): p. 639–650. [PubMed: 24997849]
12. Goetzl EJ, et al. , Neuron-Derived Plasma Exosome Proteins after Remote Traumatic Brain Injury. J Neurotrauma, 2020. 37(2): p. 382–388. [PubMed: 31441374]
13. Shetgaonkar GG, et al. , Exosomes as cell-derivative carriers in the diagnosis and treatment of central nervous system diseases. Drug Deliv Transl Res, 2021.
14. Shi M, et al. , CNS tau efflux via exosomes is likely increased in Parkinson's disease but not in Alzheimer's disease. Alzheimers Dement, 2016. 12(11): p. 1125–1131. [PubMed: 27234211]
15. Fiandaca MS, et al. , Identification of preclinical Alzheimer's disease by a profile of pathogenic proteins in neurally derived blood exosomes: A case-control study. Alzheimers Dement, 2015. 11(6): p. 600–7.e1. [PubMed: 25130657]

16. Goetzl EJ, et al. , High complement levels in astrocyte-derived exosomes of Alzheimer disease. Ann Neurol, 2018. 83(3): p. 544–552. [PubMed: 29406582]
17. Soares Martins T, et al. , Diagnostic and therapeutic potential of exosomes in Alzheimer's disease. J Neurochem, 2021. 156(2): p. 162–181. [PubMed: 32618370]
18. Zhang T, et al. , The emerging role of exosomes in Alzheimer's disease. Ageing Res Rev, 2021. 68: p. 101321. [PubMed: 33727157]
19. Shi M, et al. , New windows into the brain: Central nervous system-derived extracellular vesicles in blood. Prog Neurobiol, 2019. 175: p. 96–106. [PubMed: 30685501]
20. Kapogiannis D, et al. , Association of Extracellular Vesicle Biomarkers With Alzheimer Disease in the Baltimore Longitudinal Study of Aging. JAMA Neurol, 2019. 76(11): p. 1340–1351. [PubMed: 31305918]
21. Jia L, et al. , Concordance between the assessment of Aβ42, T-tau, and P-T181-tau in peripheral blood neuronal-derived exosomes and cerebrospinal fluid. Alzheimers Dement, 2019. 15(8): p. 1071–1080. [PubMed: 31422798]
22. Pulliam L, et al. , Plasma neuronal exosomes serve as biomarkers of cognitive impairment in HIV infection and Alzheimer's disease. J Neurovirol, 2019. 25(5): p. 702–709. [PubMed: 30610738]
23. Hong Z, et al. , Development of a Sensitive Diagnostic Assay for Parkinson Disease Quantifying α-Synuclein-Containing Extracellular Vesicles. Neurology, 2021. 96(18): p. e2332–e2345. [PubMed: 34032594]
24. Nakanishi S, et al. , Glutamate receptors: brain function and signal transduction. Brain Res Brain Res Rev, 1998. 26(2–3): p. 230–5. [PubMed: 9651535]
25. Kalsi G, et al. , Localization of the human NMDAR2D receptor subunit gene (GRIN2D) to 19q13.1-qter, the NMDAR2A subunit gene to 16p13.2 (GRIN2A), and the NMDAR2C subunit gene (GRIN2C) to 17q24-q25 using somatic cell hybrid and radiation hybrid mapping panels. Genomics, 1998. 47(3): p. 423–5. [PubMed: 9480759]
26. Alim MA, et al. , Glutamate triggers the expression of functional ionotropic and metabotropic glutamate receptors in mast cells. Cell Mol Immunol, 2021. 18(10): p. 2383–2392. [PubMed: 32313211]
27. Companys-Alemany J, et al. , A Novel NMDA Receptor Antagonist Protects against Cognitive Decline Presented by Senescent Mice. Pharmaceutics, 2020. 12(3).
28. Chang KW, et al. , Modulation of the MAPKs pathways affects Aβ-induced cognitive deficits in Alzheimer's disease via activation of α7nAChR. Neurobiol Learn Mem, 2020. 168: p. 107154. [PubMed: 31904546]
29. Jang BG, et al. , Beta-amyloid oligomers induce early loss of presynaptic proteins in primary neurons by caspase-dependent and proteasome-dependent mechanisms. Neuroreport, 2014. 25(16): p. 1281–8. [PubMed: 25275636]
30. Alzheimer's Disease Interventions: Implications of therapeutic promises amidst questions and doubts about clinically meaningful outcomes. Alzheimers Dement, 2021. 17(10): p. 1591–1594. [PubMed: 34717294]
31. Meldolesi J, Exosomes and Ectosomes in Intercellular Communication. Curr Biol, 2018. 28(8): p. R435–r444. [PubMed: 29689228]
32. Nieland L, et al. , Extracellular Vesicle-Mediated Bilateral Communication between Glioblastoma and Astrocytes. Trends Neurosci, 2021. 44(3): p. 215–226. [PubMed: 33234347]
33. Hill AF, Extracellular Vesicles and Neurodegenerative Diseases. J Neurosci, 2019. 39(47): p. 9269–9273. [PubMed: 31748282]
34. Sharma P, Schiapparelli L, and Cline HT, Exosomes function in cell-cell communication during brain circuit development. Curr Opin Neurobiol, 2013. 23(6): p. 997–1004. [PubMed: 23998929]
35. Lizarraga-Valderrama LR and Sheridan GK, Extracellular vesicles and intercellular communication in the central nervous system. FEBS Lett, 2021. 595(10): p. 1391–1410. [PubMed: 33728650]
36. Ding X, et al. , Ultrasensitive assays for detection of plasma tau and phosphorylated tau 181 in Alzheimer's disease: a systematic review and meta-analysis. Transl Neurodegener, 2021. 10(1): p. 10. [PubMed: 33712071]
37. Hwang H, et al. , GLYCOPROTEOMICS IN NEURODEGENERATIVE DISEASES. Mass Spectrometry Reviews, 2010. 29(1): p. 79–125. [PubMed: 19358229]

38. Shi M, et al. , Cerebrospinal fluid biomarkers for Parkinson disease diagnosis and progression. Ann Neurol, 2011. 69(3): p. 570–80. [PubMed: 21400565]
39. Mata IF, et al. , SNCA variant associated with Parkinson disease and plasma alpha-synuclein level. Arch Neurol, 2010. 67(11): p. 1350–6. [PubMed: 21060011]
40. Kang JH, et al. , The Alzheimer's Disease Neuroimaging Initiative 2 Biomarker Core: A review of progress and plans. Alzheimers Dement, 2015. 11(7): p. 772–91. [PubMed: 26194312]
41. Hansson O, et al. , CSF biomarkers of Alzheimer's disease concord with amyloid-β PET and predict clinical progression: A study of fully automated immunoassays in BioFINDER and ADNI cohorts. Alzheimers Dement, 2018. 14(11): p. 1470–1481. [PubMed: 29499171]
42. Shi M, et al. , Significance and confounders of peripheral DJ-1 and alpha-synuclein in Parkinson's disease. Neuroscience Letters, 2010. 480(1): p. 78–82. [PubMed: 20540987]
43. Théry C, et al. , Minimal information for studies of extracellular vesicles 2018 (MISEV2018): a position statement of the International Society for Extracellular Vesicles and update of the MISEV2014 guidelines. J Extracell Vesicles, 2018. 7(1): p. 1535750. [PubMed: 30637094]
44. Thompson AG, et al. , Extracellular vesicles in neurodegenerative disease - pathogenesis to biomarkers. Nat Rev Neurol, 2016. 12(6): p. 346–57. [PubMed: 27174238]
45. Yang Y, et al. , Cerebrospinal Fluid Particles in Alzheimer Disease and Parkinson Disease. J Neuropathol Exp Neurol, 2015. 74(7): p. 672–87. [PubMed: 26083568]
46. Howitt J and Hill AF, Exosomes in the Pathology of Neurodegenerative Diseases. J Biol Chem, 2016. 291(52): p. 26589–26597. [PubMed: 27852825]
47. Winston CN, et al. , Prediction of conversion from mild cognitive impairment to dementia with neuronally derived blood exosome protein profile. Alzheimers Dement (Amst), 2016. 3: p. 63–72. [PubMed: 27408937]
48. Goetzl EJ, et al. , Cargo proteins of plasma astrocyte-derived exosomes in Alzheimer's disease. Faseb j, 2016. 30(11): p. 3853–3859. [PubMed: 27511944]
49. Guix FX, et al. , Detection of Aggregation-Competent Tau in Neuron-Derived Extracellular Vesicles. Int J Mol Sci, 2018. 19(3).
50. Goetzl EJ, et al. , Decreased synaptic proteins in neuronal exosomes of frontotemporal dementia and Alzheimer's disease. Faseb j, 2016. 30(12): p. 4141–4148. [PubMed: 27601437]
51. Goetzl EJ, et al. , Declining levels of functionally specialized synaptic proteins in plasma neuronal exosomes with progression of Alzheimer's disease. Faseb j, 2018. 32(2): p. 888–893. [PubMed: 29025866]
52. Agliardi C, et al. , SNAP-25 in Serum Is Carried by Exosomes of Neuronal Origin and Is a Potential Biomarker of Alzheimer's Disease. Mol Neurobiol, 2019. 56(8): p. 5792–5798. [PubMed: 30680692]
53. Tatiana S, et al. , Altered level of plasma exosomes in patients with Gaucher disease. Eur J Med Genet, 2020. 63(11): p. 104038. [PubMed: 32822875]
54. Karimi N, et al. , Tetraspanins distinguish separate extracellular vesicle subpopulations in human serum and plasma - Contributions of platelet extracellular vesicles in plasma samples. J Extracell Vesicles, 2022. 11(5): p. e12213. [PubMed: 35524458]

RESEARCH IN CONTEXT

Systematic review:

The authors reviewed literature using traditional sources such as PubMed. There is a need for peripheral biomarkers for Alzheimer's disease (AD). Although several blood-based assays have been introduced, more convenient, and accessible diagnostic markers for AD are still critically needed. In particular, markers capable of reporting underlying pathological mechanisms, such as synaptic dysfunction, are badly needed.

Interpretation:

We identified NMDAR2A, a protein involved in synaptic function, as a novel marker of CNS-derived plasma extracellular vesicles (EVs). When used together with a previously identified EV marker, L1CAM, in a recently-developed flow cytometry-based technology, NMDAR2A demonstrated promising results in differentiating AD from controls, may serve as a screening tool and surrogate marker for dementia in AD diagnosis.

Future directions:

Future research will examine the utility of NMDAR2A as a marker for non-AD types of dementia, and explore its use as a marker for synaptic dysfunction.

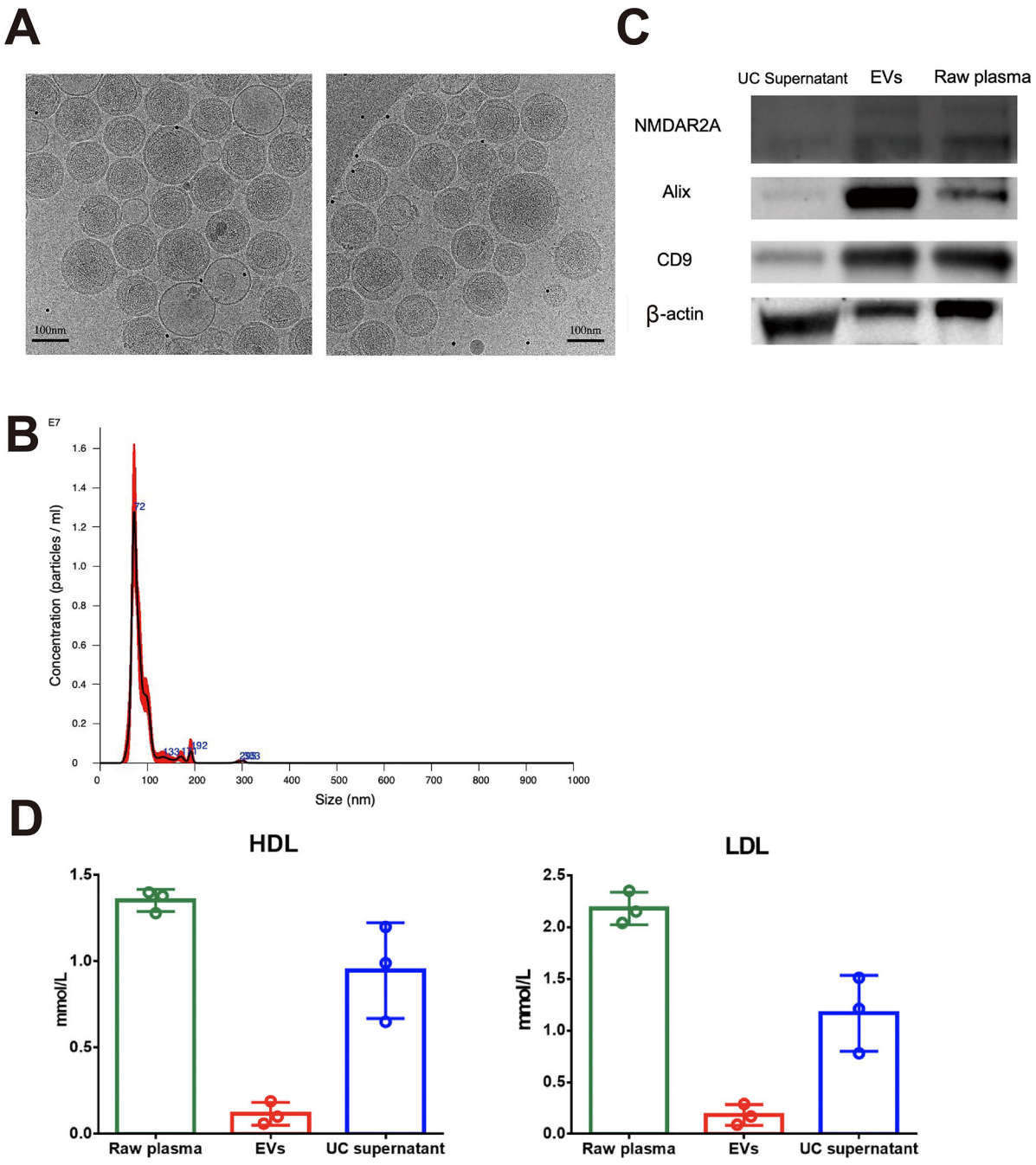

Figure 1. Characterization of EVs enriched by ultracentrifugation.

A) EV structure revealed by cryo-EM showed double layered membrane-bound vesicles with a diameter around 100 nm. B) NTA showed a population of EVs with a peak around 70 nm. C) EV and neuron marker proteins were present in the EV fraction obtained by ultracentrifugation. D) HDL and LDL were present in both EV and supernatant fractions, with the majority remaining in the supernatant.

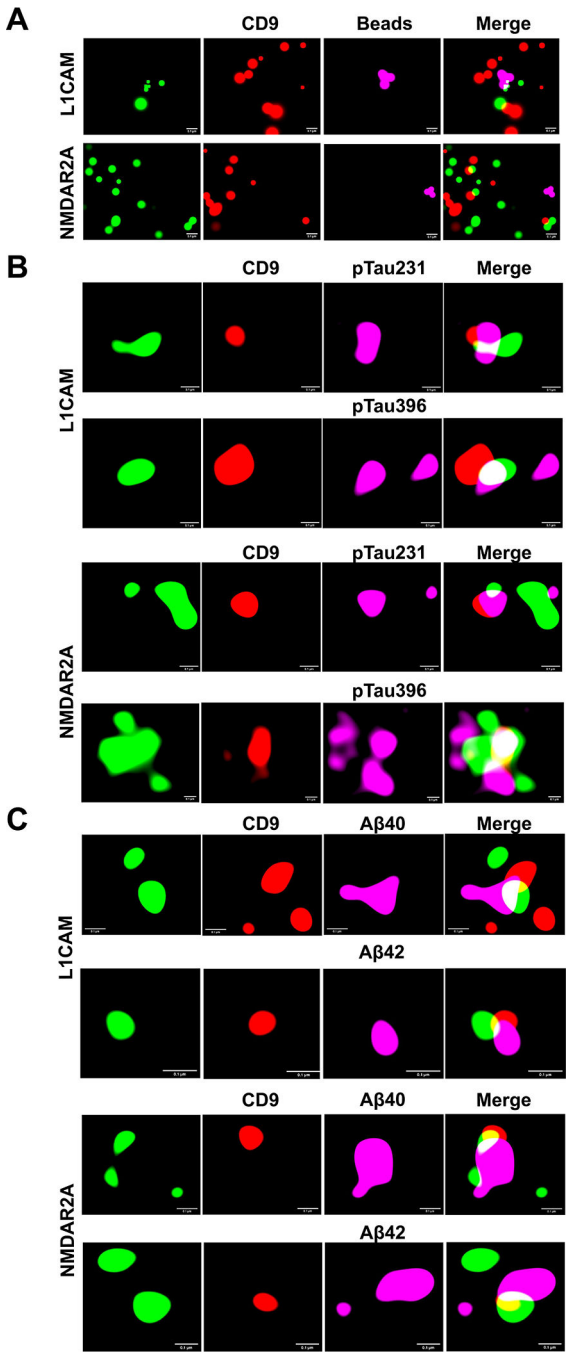

Figure 2. L1CAM and NMDAR2A are present on EV membranes.

A) STORM imaging of neuronal cell type markers (green) with EV marker CD9 (red). Fluorescent beads with a diameter of 100 nm are included to show scale. B) STORM imaging was performed to confirm L1CAM or NMDAR2A and pTau231/396 presence of EV membranes together. To confirm the EV identity of the detected signal in ultracentrifuged plasma samples, L1CAM or NMDAR2A was compared with the EV marker CD9 and pTau231/396 on the EV membranes together. Overlap of both markers with CD9 indicates their presence on EV membranes. Scale bar = 0.1 μm. C) STORM

imaging was performed to confirm L1CAM or NMDAR2A and Aβ40/Aβ42 presence of EV membranes together. To confirm the EV identity of the detected signal in ultracentrifuged plasma samples, L1CAM was compared with the EV marker CD9 and Aβ40/Aβ42 on the EV membranes together. Overlap of both markers with CD9 indicates their presence on EV membranes. Scale bar = 0.1 μm.

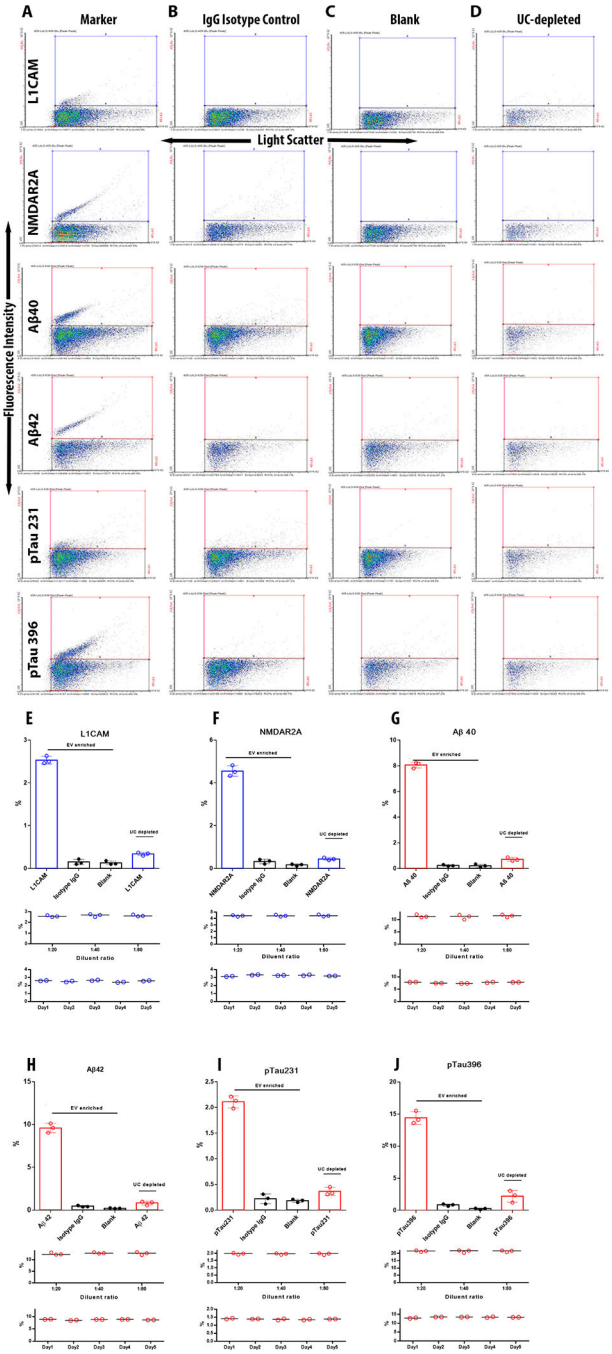

Fig. 3. Development of novel, flow cytometry-based assays for CNS and AD markers on plasma EVs.

A) Example histograms showing populations of EVs positive for each marker after labeling with fluorophore-conjugated antibody. B) Histograms of plasma samples labeled using fluorophore-conjugated IgG isotype control for the indicated marker target antibody. C) Histogram showing blank (fluorophore only, no antibody) control experiment. D) Histogram of remaining particles following depletion of EVs from plasma by ultracentrifugation. E-J) Summary data from experiments demonstrating specificity of EV assays, linearity in different dilutions of EV plasma samples, and stability of reference plasma (2 replicates run

each day on 5 separate days of the experiment) for E) L1CAM, F) NMDAR2A, G) Aβ40, H) Aβ42, I) pTau 231, J) pTau 396

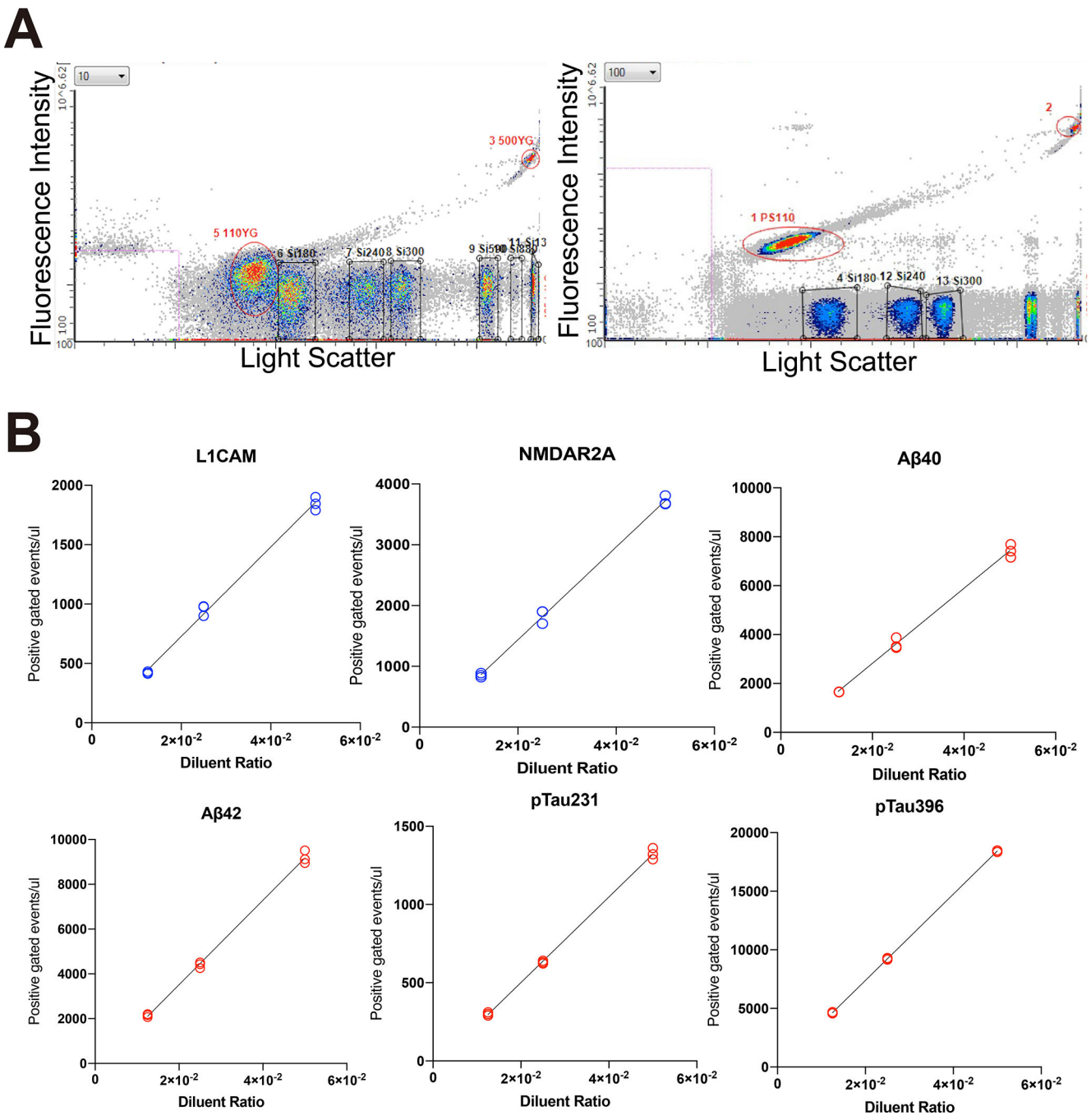

Figure 4. Apogee flow cytometry.

A) Apogee flow cytometry was regularly calibrated using a set of standard beads. B) Sample dilution showing linearity to exclude detection of excess doublets.

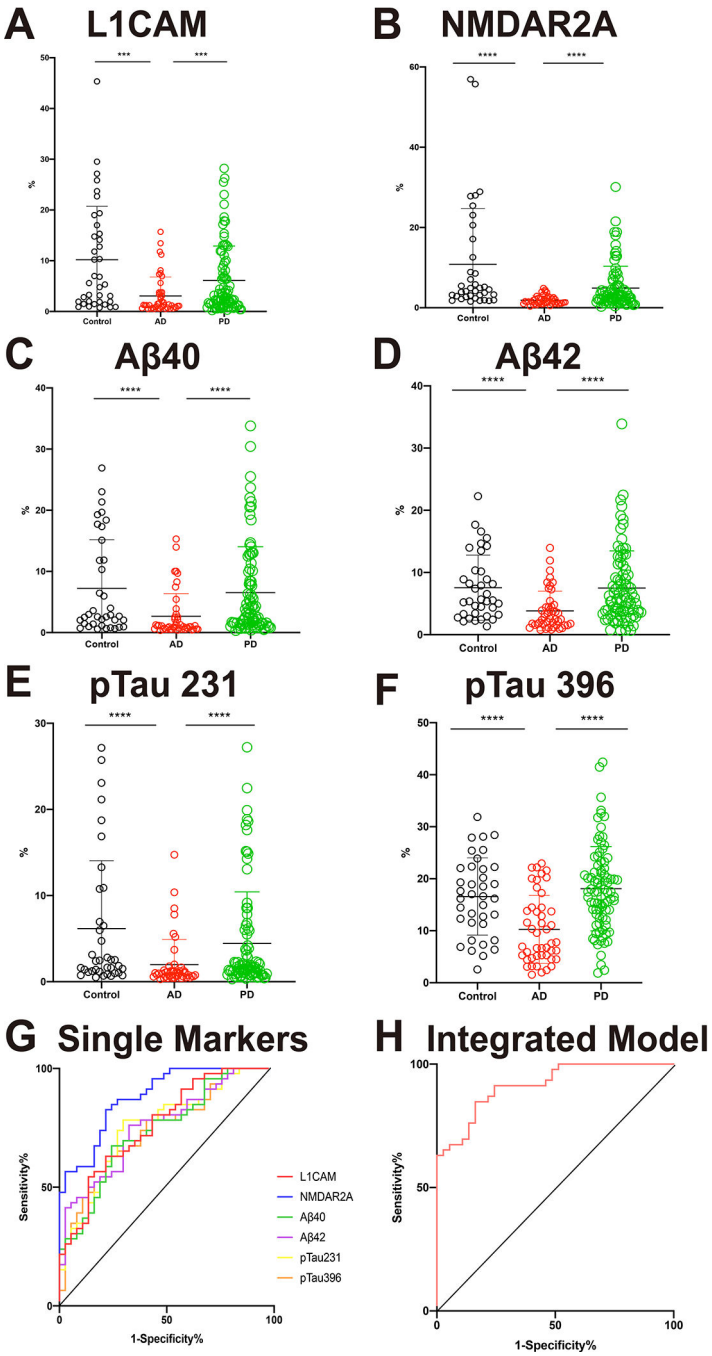

Fig. 5. Performance of CNS-derived EV markers in the discovery cohort.

A) The percentage of L1CAM+ EVs was significantly lower in AD than in PD and healthy control. B) The percentage of NMDAR2A+ EVs was significantly lower in AD than in healthy control, and trended lower than in PD. AD subjects also had lower percent positive than healthy control or PD patients for C) Aβ 40, D) Aβ42, E) pTau 231, and F) pTau 396. G) When individual markers were used to distinguish AD from control, their performance was moderate. ROC curves showing separation of AD from control using EVs carrying L1CAM, NMDAR2A, Aβ40, Aβ42, pTau 231, and pTau 396 H) Integrative

model including all EV markers distinguishes AD from control. *p<0.05 compared to AD. **p<0.01 compared to AD. ***p<0.001 compared to AD. Kruskal-Wallis test followed by Dunnett's multiple comparisons test.

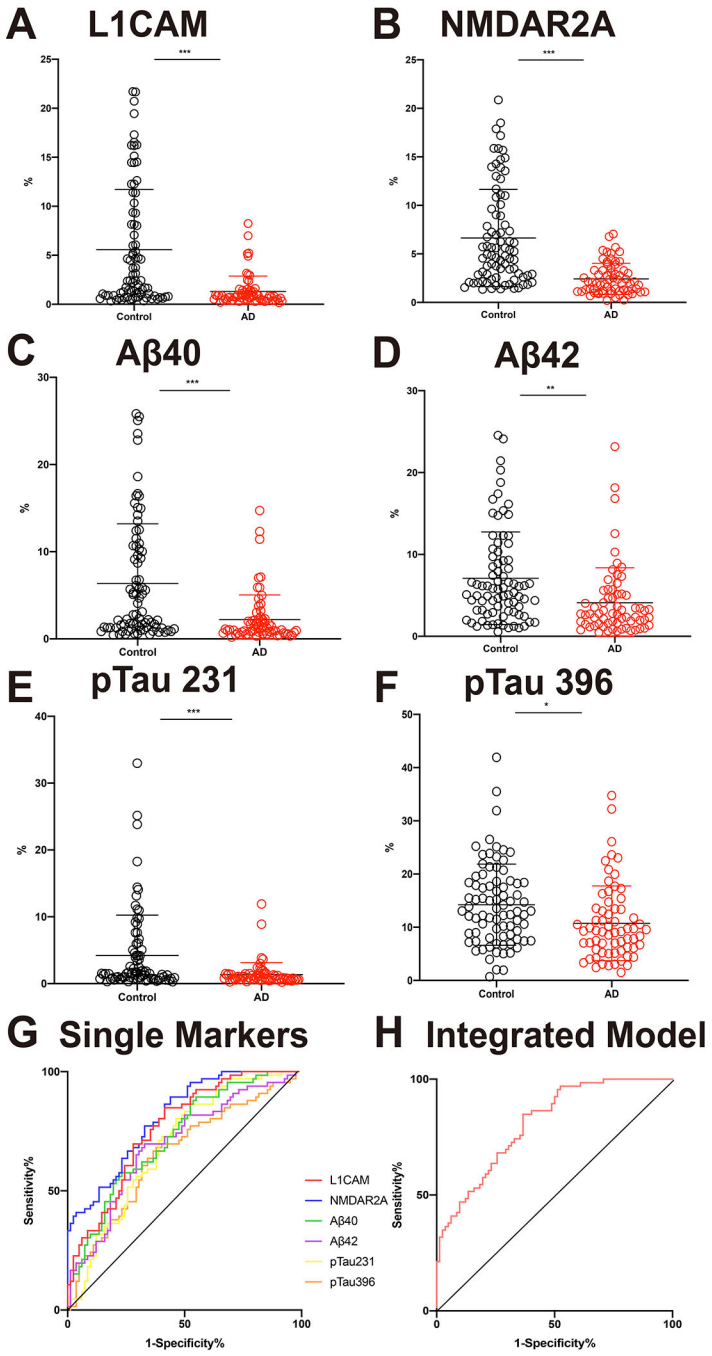

Fig. 6. Performance of CNS-derived EV markers in the validation cohort.

The percentages of A) L1CAM+, B) NMDAR2A+, C) Aβ40+, D) Aβ42+, E) pTau 231+, and F) pTau 396+ EVs were significantly lower in AD than in control. G) When individual markers were used to distinguish AD from control, their performance was moderate. ROC curves showing separation of AD from control using EVs carrying L1CAM, NMDAR2A, Aβ40, Aβ42, pTau 231, and pTau 396. H) Integrative model including all EV markers distinguishes AD from control. *p<0.05, **p<0.01, ***p<0.001, Mann–Whitney test.

Table 1.

Demographics and biomarker levels for two cohorts.

	Discovery Cohort			ADNI Cohort	
	Control	**AD**	**PD**	**Control**	**AD**
Number	32	45	84	82	66
Age (years)					
Mean±S.D.	69.97±8.59	68.74±9.48	67.59±5.59	74.04±5.65	75.53±8.16
Range	55–88	52–85	57–83	62–90	56–90
EV markers (percent positive ± S.D.) in CSF-confirmed cases					
L1CAM	10.71±10.90 ***	3.05±3.78	6.12±6.78 *	5.57±6.14 ***	1.30±1.57
NMDAR2A	11.46±14.52 ***	1.90±1.09	4.91±5.44	6.64±5.01 ***	2.42±1.61
Aβ40	7.57±8.14 **	2.70±3.75	6.53±7.51 **	6.37±6.83 ***	2.20±2.84
Aβ42	7.94±5.42 **	3.87±3.19	7.50±5.96 ***	7.09±5.65 **	4.10±4.26
pTau 231	6.54±8.21 **	2.00±2.96	4.43±6.0 *	4.21±6.05 ***	1.35±1.78
pTau 396	16.81±7.64 ***	10.29±6.60	18.08±8.12 ***	14.24±7.62 *	10.73±7.02

* p<0.05 compared to AD.

** p<0.01 compared to AD.

*** p<0.001 compared to AD.

ANOVA followed by Dunnett's multiple comparisons test. Aβ40, amyloid beta 1–40; Aβ42, amyloid beta 1–42; L1CAM, L1 cell adhesion molecule; NMDAR2A, N-methyl-D-aspartate receptor 2A; pTau231, tau phosphorylated at T231; pTau396, tau phosphorylated at S236

Table 2.

Correlation matrix of EV markers and age.

	Age	L1CAM	NMDAR2A	Aβ 40	Aβ 42	231	396
Age		0.076 0.36	0.061 0.46	0.053 0.52	0.058 0.524	0.088 0.29	0.033 0.69
L1CAM	−0.066 0.41		**0.879** **0.000**	**0.790** **0.000**	**0.565** **0.000**	**0.762** **0.000**	**0.376** **0.000**
NMDAR2A	0.046 0.57	**0.760** **0.000**		**0.689** **0.000**	**0.518** **0.000**	**0.674** **0.000**	**0.387** **0.000**
Aβ 40	−0.117 0.14	**0.816** **0.000**	**0.551** **0.000**		**0.852** **0.000**	**0.809** **0.000**	**0.0629** **0.000**
Aβ 42	0.23 0.23	**0.599** **0.000**	**0.352** **0.000**	**0.876** **0.000**		**0.676** **0.000**	**0.826** **0.000**
231	−0.092 0.25	**0.673** **0.000**	**0.766** **0.000**	**0.750** **0.000**	**0.620** **0.000**		**0.378** **0.000**
396	−0.107 0.177	**0.370** **0.000**	**0.290** **0.000**	**0.515** **0.000**	**0.648** **0.000**	**0.487** **0.000**	

Blue boxes show correlations of markers with age, and correlations between markers, in the discovery cohort. Red boxes show the same correlations in the ADNI validation cohort.

Table 3.

Areas under the curve for ROC analyses

Comparison	Marker	AUC	95% CI	Cut-off
Discovery Cohort				
AD vs Control	L1CAM	0.763	0.662–0.865	5.62%
	NMDAR2A	0.882	0.813–0.951	2.20%
	Aβ40	0.741	0.635–0.846	5.54%
	Aβ42	0.759	0.657–0.860	9.18%
	pTau 231	0.758	0.654–0.862	2.00%
	pTau 396	0.740	0.634–0.846	10.34%
AD vs PD	L1CAM	0.660	0.564–0.757	5.08%
	NMDAR2A	0.729	0.643–0.814	2.10%
	Aβ40	0.738	0.647–0.830	5.64%
	Aβ42	0.727	0.636–0.817	9.91%
	pTau 231	0.704	0.611–0.798	2.41%
	pTau 396	0.773	0.686–0.859	11.51%
Validation Cohort (ADNI)				
AD vs Control	L1CAM	0.762	0.687–0.838	5.01%
	NMDAR2A	0.809	0.742–0.876	3.47%
	Aβ40	0.725	0.644–0.805	5.59%
	Aβ42	0.696	0.611–0.781	5.73%
	pTau 231	0.693	0.609–0.777	2.40%
	pTau 396	0.655	0.566–0.744	17.28%